UC Berkeley
UC Berkeley Previously Published Works

Title

What Is the Structure of the Naphthalene–Benzene Heterodimer Radical Cation? Binding Energy, Charge Delocalization, and Unexpected Charge-Transfer Interaction in Stacked Dimer and Trimer Radical Cations

Permalink

Journal

ISSN

Authors

Attah, Isaac K
Platt, Sean P
Meot-Ner, Michael
et al.

Publication Date

DOI

What is the Structure of the Naphthalene-Benzene Heterodimer Radical Cation? Binding Energy, Charge Delocalization and Unexpected Charge Transfer Interaction in Stacked Dimer and Trimer Radical Cations

Journal:	*The Journal of Physical Chemistry Letters*
Manuscript ID:	jz-2014-02438x.R2
Manuscript Type:	Letter
Date Submitted by the Author:	06-Feb-2015
Complete List of Authors:	Attah, Isaac; Virginia Commonwealth University, Chemistry Platt, Sean; Virginia Commonwealth University, Chemistry Mautner, Michael; Virginia commonwealth University, Chemistry El-Shall, M. Samy; Virginia Commonwealth University, Dept of Chemistry Peverati, Roberto; UC Berkeley, Department of Chemistry and Supercomputing Institute Head-Gordon, Martin; University of California, Berkeley, Chemistry

SCHOLARONE™
Manuscripts

1
2
3
4
5
6
7
8
9
10
11
12
13
14
15
16
17
18
19
20
21
22
23
24
25
26
27
28
29
30
31
32
33
34
35
36
37
38
39
40
41
42
43
44
45
46
47
48
49
50
51
52
53
54
55
56
57
58
59
60

What is the Structure of the Naphthalene-Benzene Heterodimer Radical Cation? Binding Energy, Charge Delocalization and Unexpected Charge Transfer Interaction in Stacked Dimer and Trimer Radical Cations

Isaac K. Attah, Sean P. Platt, Michael Meot-Ner (Mautner), and M. Samy El-Shall*

Department of Chemistry, Virginia Commonwealth University, Richmond, VA 23284-2006

Roberto Peverati and Martin Head-Gordon*

Department of Chemistry, University of California, Berkeley, California, 94720 USA and Chemical Sciences Division, Lawrence Berkeley National Laboratory, Berkeley, California, 94720

Abstract

The binding energy of the naphthalene$^{+\bullet}$(benzene) heterodimer cation has been determined as 7.9 ± 1 kcal/mol for $C_{10}H_8^{+\bullet}(C_6H_6)$ and 8.1 ± 1 kcal/mol for $C_{10}H_8^{+\bullet}(C_6D_6)$ by equilibrium thermochemical measurements using the mass-selected drift cell technique. A second benzene molecule binds to the $C_{10}H_8^{+\bullet}(C_6D_6)$ dimer with essentially the same energy (8.4 ± 1 kcal/mol) suggesting that the two benzene molecules are stacked on opposite sides of the naphthalene cation in the $(C_6D_6)C_{10}H_8^{+\bullet}(C_6D_6)$ heterotrimer. The lowest energy isomers of the $C_{10}H_8^{+\bullet}(C_6D_6)$ and $(C_6D_6)C_{10}H_8^{+\bullet}(C_6D_6)$ dimer and trimer calculated using the M11/cc-pVTZ method have parallel stacked structures with enthalpies of binding ($-\Delta H°$) of 8.4 and 9.0 kcal/mol, respectively in excellent agreement with the experimental values. The stacked face-to-face class of isomers is calculated to have substantial charge-transfer stabilization of about 45% of the total interaction energy in spite of the large difference between the ionization energies of benzene and naphthalene. Similarly, significant delocalization of the positive charge is found among all three fragments of the $(C_6D_6)C_{10}H_8^{+\bullet}(C_6D_6)$ heterotrimer thus leaving only 46% of the total charge on the central naphthalene moiety. This unexpectedly high charge-transfer component results in activating two benzene molecules in the naphthalene$^{+\bullet}$(benzene)$_2$ heterotrimer cation to associate with a third benzene molecule at 219 K to form a benzene trimer cation and a neutral naphthalene molecule. The global minimum of the $C_{10}H_8^{+\bullet}(C_6H_6)_2$ heterotrimer is found to be the one where the naphthalene cation is sandwiched between two benzene molecules. It is remarkable, and rather unusual, that the binding energy of the second benzene molecule slightly exceeds that of the first. This is attributed to the enhanced charge transfer interaction in the stacked trimer radical cation.

TOC Graphic

$C_{10}H_8^{+\bullet}(C_6H_6)$ $C_{10}H_8^{+\bullet}(C_6H_6)_2$
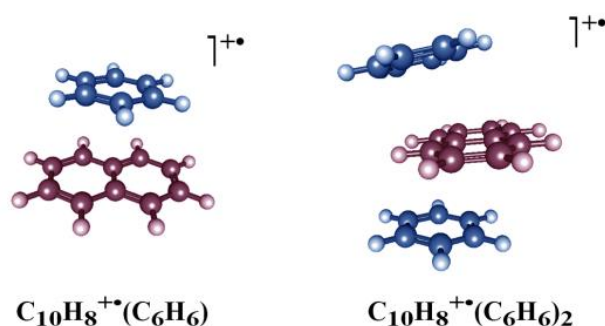
KEYWORDS: Dimer Radical Cations, Stacked Dimers, Naphtalene-Benzene Dimer Cation, Charge Transfer, Charge Delocalization

Dimer radical cations of aromatic and polycyclic aromatic molecules are of fundamental importance in chemistry, biochemistry and materials science since they constitute the smallest intermolecular units that carry a delocalized positive charge and thus provide the basis for photoconductivity and ferromagnetism in organic materials.[1-6] These interactions play critical roles in other diverse areas such as protein structures, base pair stacking in DNA, drug design, and crystal packing of aromatic molecules.[7-10] Dimer cations of polycyclic aromatics may also play important roles in astrochemistry, where they may be responsible for much of the interstellar extended red emission at 450-899 nm.[11-14]

In homodimer radical cations such as benzene and naphthalene dimers ((Bz.Bz)$^{+\bullet}$ and (Naph.Naph)$^{+\bullet}$, respectively) the unpaired electron is considered to be equally distributed between the two moieties providing extra charge resonance stabilization in addition to the ion-induced dipole and dispersion interactions.[6] The binding energy of a mass-selected and isomer specific (Bz.Bz)$^{+\bullet}$ has been recently measured as 17.6±1 and 17.4±1 kcal/mol, for the $(C_6H_6)_2^{+\bullet}$ and $(C_6D_6)_2^{+\bullet}$ systems, respectively.[15] These values are similar to the value (17.0 kcal/mol) reported earlier by Meot-Ner *et al* using pulsed high pressure mass spectrometry.[16] The large binding energy of the (Bz.Bz)$^{+\bullet}$ dimer suggests a significant contribution from a charge resonance interaction which is at a maximum in sandwich-like structures.[15-19] Therefore, the benzene dimer cation is considered to adopt a parallel sandwich configuration on the basis of maximizing the charge transfer resonance interaction $C_6H_6^+.C_6H_6 \rightleftharpoons C_6H_6.C_6H_6^+$.[15,16] Density functional theory calculations, at an all-electron level and without any symmetry constraint, predicts that the dimer cation has two nearly degenerate ground state structures with the sandwich configuration more stable than the T-configuration by only 1.6 kcal/mol.[20] The ion mobility experiment indicates that only one structure is observed for the mass-selected dimer cation with a measured collision cross section in helium of 71 Å^2 at room temperature in good agreement (within 2.4%) with the calculated cross section for the sandwich dimer.[20]

Knowledge of the structure and binding energy of the naphthalene$^{+\bullet}$.benzene heterodimer radical cation is essential in order to understand the effect of charge delocalization in the larger naphthalene cation, as compared to the benzene cation, on the bonding to the neutral benzene molecule and on the contribution of charge transfer interaction to the binding energy of the heterodimer. It has been shown that the dissociation energies of the heterodimer radical cations decrease with increasing the difference in the IE's of the component molecules (ΔIE).[16-18] This correlation was reported in several series of dimers containing benzene, aniline

2

and methylnaphthalene radical cations and different neutral molecules.[16-18] Based on this correlation, charge transfer interaction in the naphthalene$^{+\bullet}$.benzene heterodimer is expected to be very small due to the large difference in the IEs between benzene and naphthalene (1.1 eV).[21] However, unambiguous determination of the charge transfer contribution to the overall binding energy of the heterodimer may not be possible without knowing the most likely structure of the heterodimer. This is mostly due to the presence of different structural isomers of the heterodimer with essentially similar binding energies but with different contributions from the interaction energy components such as dispersion, polarization, charge transfer, and charge resonance interactions. Here, we report the first experimental binding energy measurements of the [Naph.Bz]$^{+\bullet}$ and [Naph.(Bz)$_2$]$^{+\bullet}$ heterodimer and trimer, respectively using the mass-selected drift cell technique. In addition we report high level theoretical calculations to characterize the potential energy surface of the interaction, identify the main minima, and quantify the nature of the interaction in the [Naph.Bz]$^{+\bullet}$ and [Naph.(Bz)$_2$]$^{+\bullet}$ heterodimer and trimer radical cations, respectively. The results provide direct evidence for significant charge transfer interactions between the naphthalene radical cation and benzene molecules in the stacked dimer and trimer in spite the large difference in the ionization energies of naphthalene and benzene. This unexpected charge transfer interaction is shown to drive an exchange reaction with a benzene molecule to convert the [Naph.(Bz)$_2$]$^{+\bullet}$ heterodimer into the more stable benzene homotrimer (Bz)$_3$$^{+\bullet}$ where charge resonance interaction can provide additional stabilization energy.

The experiments were performed using the VCU mass-selected ion mobility spectrometer (Schematic is given in **Figure S1**, Supporting Information). The details of the instrument can be found in several publications[15,22,23] and only a brief description of the experimental procedure is given here. Mass-selected C$_{10}$H$_8$$^{+\bullet}$ ions (generated by electron impact ionization of naphthalene vapor) are injected (in 20 –30 μsec pulses) into the drift cell containing 1.0 Torr helium and 0.10 - 0.35 Torr of benzene (C$_6$H$_6$ or C$_6$D$_6$) vapor. The temperature of the drift cell can be controlled to better than ±1K using six temperature controllers. The reaction products can be identified by scanning a second quadrupole mass filter located coaxially after the drift cell. The injection energies used in the experiments (10–12 eV laboratory frame, depending on the pressure in the drift cell) are slightly above the minimum energies required to introduce the naphthalene ions against the counter flow of the gas escaping from the cell. Most of the ion thermalization occurs outside the cell entrance by collisions with the helium atoms and benzene molecules escaping from the cell entrance orifice.

3

At a cell pressure of 0.2 Torr, the number of collisions that the naphthalene ion encounters within the 1.5 millisecond residence time inside the cell is about 10^4 collisions, which is sufficient to ensure efficient thermalization of the ions. The ion intensity ratio $C_{10}H_8^{+\bullet}(C_6H_6)/C_{10}H_8^{+\bullet}$ is measured from the ion intensity peaks as a function of decreasing cell drift field corresponding to increasing reaction time, and equilibrium is achieved when a constant ratio is obtained. Equilibrium constants are then calculated from $K = [I(C_{10}H_8^{+\bullet}(C_6H_6))/I(C_{10}H_8^{+\bullet}) \, P(benzene)]$ where I is the ion intensity taken from the mass spectrum and P(benzene) is the partial pressure of benzene in the drift cell. All the equilibrium experiments at different temperatures are conducted at correspondingly low drift fields and long residence times. The measured equilibrium constant is independent of the applied field across the drift cell in the low field region. The equilibrium constant measured as a function of temperature yields $\Delta H°$ and $\Delta S°$ from the van't Hoff equation $[\ln K = -\Delta H°/RT + \Delta S°/R]$.

       Figure 1 displays the mass spectra obtained following the injection of the mass-selected naphthalene cation $(C_{10}H_8^{+\bullet})$ into the drift cell pure helium or helium-benzene (C_6D_6) gas mixtures. Similar results were obtained for injecting the naphthalene cation into helium-C_6H_6 gas mixtures (**Figure S2**, Supporting Information). In the presence of 0.35 Torr C_6D_6 vapor in the drift cell at 269 K, the naphthalene$^{+\bullet}$.benzene heterodimer $((Naph.Bz) = C_{10}H_8^{+\bullet}(C_6D_6))$, along with the (benzene)$_2^{+\bullet}$ homodimer $((Bz)_2 = (C_6D_6)_2)$ are observed as shown in Fig. 1(b). Although no dissociation products of the naphthalene ion are observed (Fig. 1(a)) consistent with the low injection energy used, the observation of the small ion intensity of the (benzene)$_2^{+\bullet}$ suggests direct ionization of a small amount of the benzene molecules in the cell by the injection energy. As the temperature decreases the ion intensity of the (Naph$^{+\bullet}$.Bz) dimer increases (Fig. 1(c)), and at 229 K small peaks corresponding to the Naph$^{+\bullet}$(Bz)$_2$ heterotrimer and the benzene homotrimer (Bz)$_3^{+\bullet}$ are formed as shown in Fig. 1(d). At the lowest possible temperature in the drift cell of 219 K (just before the benzene vapor freezes out), a significant decrease in the intensity of the Naph$^{+\bullet}$(Bz) ion and a large increase in the intensities of the Naph$^{+\bullet}$(Bz)$_2$ and (Bz)$_3^{+\bullet}$ ions are observed as shown in Fig. 1(e).
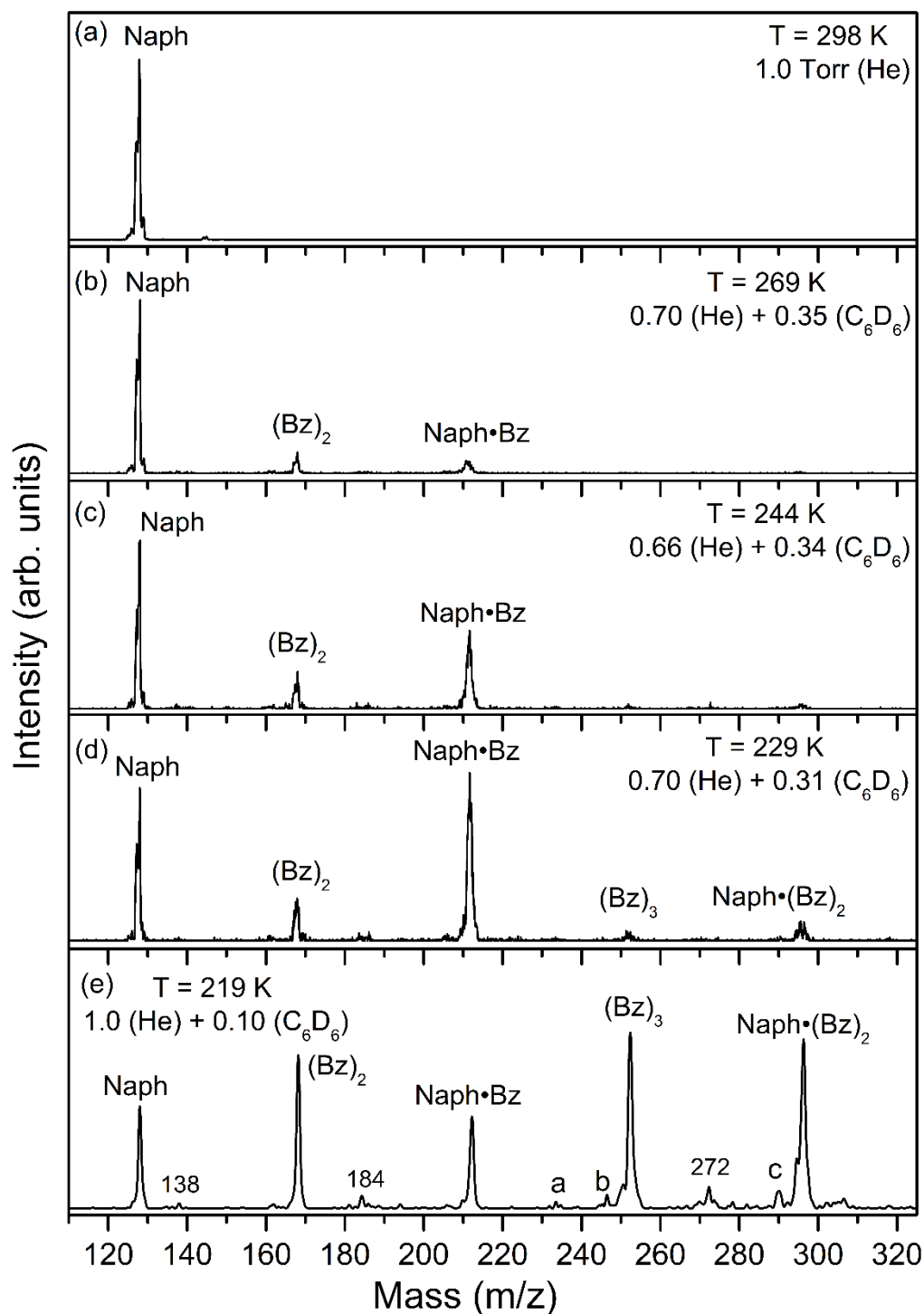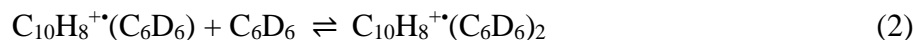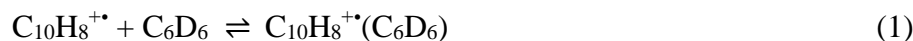
Figure 1. Mass spectra resulting from the injection of the mass-selected naphthalene radical cation ($C_{10}H_8^{+\bullet}$, Naph) into helium gas or helium-benzene (C_6D_6) vapor mixture at different temperatures and pressures as indicated. Peaks labelled a (m/z 234 = $(C_6H_6)_3$), b (m/z 246 = $(C_6D_6)_2(C_6H_6)^{+\bullet}$), and c (m/z 290 = $(C_{10}H_8^{+\bullet}(C_6D_6)(C_6H_6))$) in panel (e) are due to isotope contamination (C_6H_6) in the C_6D_6 sample. The m/z peaks 138, 184 and 272 in panel (e) are due to pump oil impurities that tend to be observed in the drift cell at high pressures and low temperatures.

The observed association reactions of benzene with the naphthalene cation are represented by equations (1) and (2):

$$C_{10}H_8^{+\bullet} + C_6D_6 \rightleftharpoons C_{10}H_8^{+\bullet}(C_6D_6) \tag{1}$$

$$C_{10}H_8^{+\bullet}(C_6D_6) + C_6D_6 \rightleftharpoons C_{10}H_8^{+\bullet}(C_6D_6)_2 \tag{2}$$

The equilibrium constants for reaction (1) measured at different temperatures for both C_6H_6 and C_6D_6 yield the van't Hoff plots for the formation of the $C_{10}H_8^{+\bullet}(C_6H_6)$ and $C_{10}H_8^{+\bullet}(C_6D_6)$ dimers, respectively as shown in **Figures 2(a) and 2(b),** respectively. The measured equilibrium constants and van't Hoff plots are duplicated at least three times, and the estimated errors in ΔH^o and ΔS^o values are obtained from standard deviations of van't Hoff plots and from typical uncertainties in thermochemical equilibrium studies. The resulting $-\Delta H^o$ and $-\Delta S^o$ values for the formation of $C_{10}H_8^{+\bullet}(C_6H_6)$ are 7.9 ±1 kcal/mol and 18.7 ±2 cal/mol K, respectively as shown in Fig. 2(a). The corresponding $-\Delta H^o$ and $-\Delta S^o$ values for the formation of $C_{10}H_8^{+\bullet}(C_6D_6)$ are 8.1 ±1 kcal/mol and 20.2 ±2 cal/mol K, respectively as shown in Fig. 2(b). It is clear that the isotope effects on the enthalpy and entropy changes are smaller than the usual experimental uncertainties of ±1 kcal mol^{-1} and ±2 cal/mol K, respectively for such measurements.
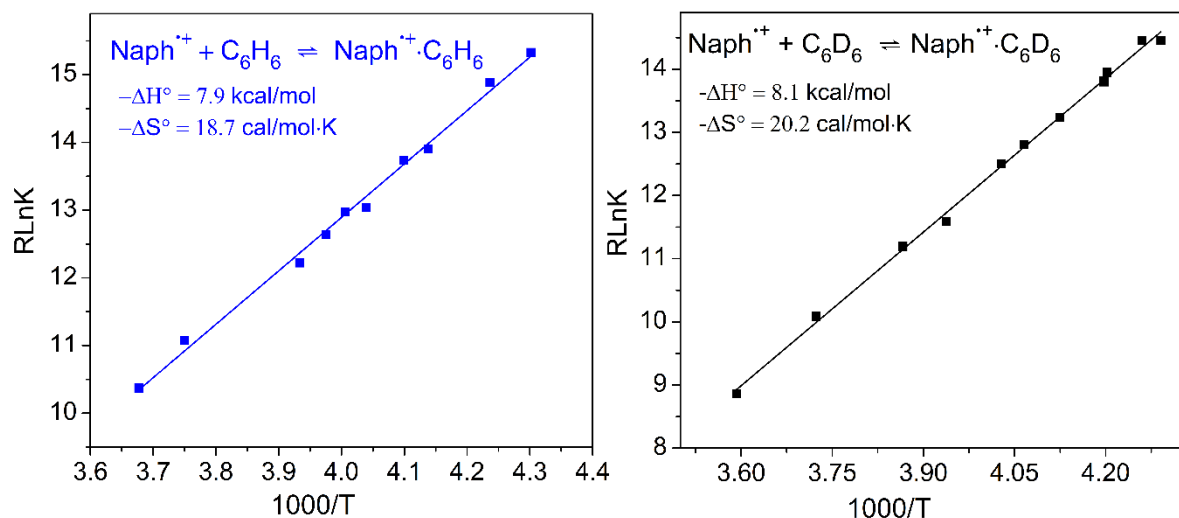

Figure 2. van't Hoff plots for formation of $C_{10}H_8^{+\bullet}(C_6H_6)$ (Left) and $C_{10}H_8^{+\bullet}(C_6D_6)$ (Right) heterodimer cations. Error estimates are ±1 kcal/mol and ±2 cal/mol K for ΔH^o and ΔS^o, respectively.

6

Because of the very small temperature range where the $C_{10}H_8^{+\bullet}(C_6D_6)_2$ could be observed (215-219 K), it was not possible to measure a van't Hoff plot for the formation of the $C_{10}H_8^{+\bullet}(C_6D_6)_2$ heterotrimer. Alternatively, we measured ΔG^o the association reaction (2) at 219 K as -4.2 kcal/mol, and assuming a ΔS^o of -19 cal/mol K, we can estimate $-\Delta H^o$ for association of the second benzene molecule to the $C_{10}H_8^{+\bullet}(C_6D_6)$ dimer as 8.4 kcal/mol. Interestingly, this value is similar to the binding energy of benzene to the naphthalene cation in the $Naph^{+\bullet}(Bz)$ heterodimer, and it suggests that the second benzene molecule has a similar interaction with the naphthalene cation as the first benzene molecule. A possible structure that could explain this binding behavior is the one where the naphthalene cation is sandwiched between two benzene molecules. This structure will be tested by the theoretical calculations below.

The mass spectrum at 219 K shown in Fig. 1(e) suggests the simultaneous formation of the benzene homotrimer $(Bz)_3^{+\bullet}$ with the formation of the $Naph^{+\bullet}(Bz)_2$ heterotrimer. The formation of the benzene trimer cation $(Bz)_3^{+\bullet}$ can be explained by the exchange reaction (3).
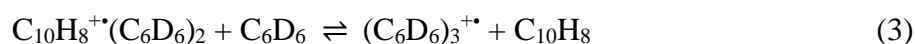
$$C_{10}H_8^{+\bullet}(C_6D_6)_2 + C_6D_6 \rightleftharpoons (C_6D_6)_3^{+\bullet} + C_{10}H_8 \qquad (3)$$

Because of the higher IE of benzene (9.2 eV) relative to that of naphthalene (8.1 eV)[21], charge transfer (CT) within the $C_{10}H_8^{+\bullet}(C_6D_6)$ heterodimer is energetically unfavorable. Also, charge transfer from $C_{10}H_8^{+\bullet}$ to the benzene dimer $(C_6D_6)_2$ is unlikely since the IE of the benzene dimer (8.4 - 8.5 eV)[34-36] is still higher than that of naphthalene (8.1 eV). However, the generation of the benzene trimer cation $(C_6D_6)_3^{+\bullet}$ at 219 K could be explained by Associative Charge Transfer (ACT) reactions observed previously in the benzene$^{+\bullet}$/propene system at room temperature[37] and in the benzene$^{+\bullet}$/acetylene system at low temperatures.[21,38] In the present system, partial charge transfer from the naphthalene ion to the two benzene molecules in $C_{10}H_8^{+\bullet}(C_6D_6)_2$ drives the exchange reaction (3) to form a benzene trimer cation, whose binding energy (7.8 kcal/mol)[39] is higher than the binding of benzene to $C_{10}H_8^{+\bullet}(C_6D_6)_2$ to form $C_{10}H_8^{+\bullet}(C_6D_6)_3$. Also, because the IE of benzene trimer is lower than that of the benzene dimer,[40-42] CT from $C_{10}H_8^{+\bullet}$ to the benzene trimer in $C_{10}H_8^{+\bullet}(C_6D_6)_3$ could become thermoneutral or even exothermic. In fact, using the measured binding energy of the third benzene molecule to the benzene dimer cation (7.8 kcal/mol)[39] the hypothetical reaction: $[C_{10}H_8^{+\bullet} + 3\ C_6D_6 \rightarrow (C_6D_6)_3^{+\bullet} + C_{10}H_8]$ is calculated to be an exothermic by about 3 kcal/mol. This suggests that reaction (3) could occur at low temperature such as 219 K to generate the

7

$(Bz)_3^{+\bullet}$, and then some of the $(Bz)_3^{+\bullet}$ product may dissociate to form $(Bz)_2^{+\bullet}$ as observed in Fig. 1(e).

The measured enthalpy of binding of the naphthalene$^{+\bullet}$.benzene heterodimer (8 kcal/mol) is significantly smaller than that of the (benzene)$_2^{+\bullet}$ homodimer (17 kcal/mol)[15,16] and also of the (naphthalene)$_2^{+\bullet}$ homodimer (17.8 kcal/mol)[16]. This could be explained by two factors: (1) the delocalization of the charge on the larger naphthalene cation as compared to the benzene cation, could lead to weaker charge-induced dipole interactions with the neutral benzene molecule, and (2) the lack of charge resonance interaction in the naphthalene$^{+\bullet}$.benzene heterodimer as a result of the large difference in the IEs between benzene and naphthalene (1.1 eV).[21] To understand the nature of bonding in the naphthalene$^{+\bullet}$.benzene heterodimer and characterize the potential energy surface of the interaction, we carried out DFT calculations using the cc-pVTZ basis set and the results are discussed below.

For the identification of structural minima we used a methodology that combines quenching *ab-initio* molecular dynamics (QAIMD) starting from random initial orientations, followed by gradient-based local optimizations with density functional theory (DFT) using the cc-pVTZ basis set. The accuracy of the basis set was checked by calculations with the larger aug-cc-pVTZ basis set. The DFT results with the M06-2X,[24] M11,[25] and ωB97X-V[26] exchange-correlation functionals were also compared to more advanced wave function techniques such as Møller-Plesset perturbation theory (MP2),[27] spin-component-scaled MP2 (SCS-MP2),[28] and orbital-optimized opposite spin MP2 (O2)[29] using single point energy calculations. To study the nature of the bonds we also used the absolutely-localized molecular orbitals energy decomposition and charge-transfer analyses, ALMO-EDA and ALMO-CTA.[30-32] All calculations were performed with the Q-Chem 4 quantum chemistry code.[33]

The potential energy surface for the interaction is relatively shallow, with many local minima and low transition barriers. We identified a total of 15 minima, which may be divided into three categories, according to the angle between the planes of the naphthalene and benzene molecules as shown **Figure 3**. In **Table S1** (Supporting Information), we report the 15 identified isomers, ordered according to their interaction energy within each group (electronic energies at 0K), along with the inter-plane angle and the closest contact distance for each isomer. The coordinates of the atoms for each structure are also reported in the Tables of Coordinates in the Supporting Information.
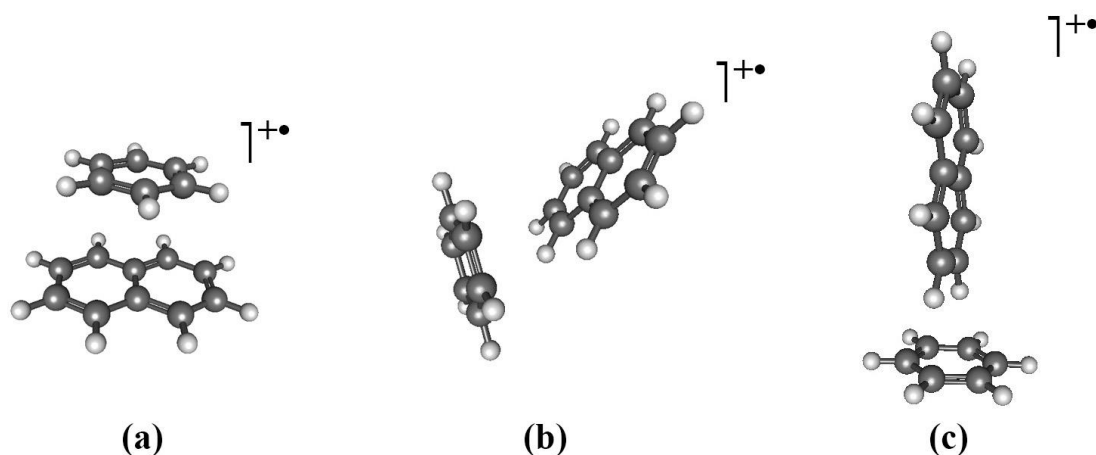
8

Figure 3. The three classes of isomers of the naphthalene$^{+\bullet}$.benzene heterodimer: (a) face-to-face, (b) V-shaped and (c) face-to-side. In each case, the lowest energy isomer is depicted.

The analysis of the calculations shows good qualitative agreement between the recently developed range-separated functionals, M11 and ωB97X-V, and the wave function methods, while in terms of the basis set, the results with the cc-pVTZ basis are essentially identical to the results with the more expensive aug-cc-pVTZ basis (the largest difference is 0.06 kcal/mol). For these reasons we base our discussion on the M11/cc-pVTZ results, though we report results for all methodologies used in **Table S2** (Supporting Information). The calculations predict a face-to-face isomer to be the global minimum, with a V-shaped isomer very close in energy, only 0.3 kcal/mol higher than the global minimum. These nearly identical relative energies of the local minima indicate a very flat potential energy surface for encounter of Bz and Naph$^{+\bullet}$. If we consider all structures within the chemically significant margin of 1 kcal/mol from the lowest energy structure, we have at least five face-to-face structures and all six V-shaped structures. A slightly more significant margin is found for the face-to-side class, whose lowest energy isomer is 1.2 kcal/mol higher than the global minimum. Because the potential energy surface is very flat, we expect the transition barriers between these minima to be very small, and the system will be able to explore multiple minima under experimental conditions.

To compare the calculated binding energies to the experiment, we estimated the thermochemical corrections and calculated the enthalpies of reaction at 298K. The agreement between the M11/cc-pVTZ calculated binding energy of 8.4 kcal/mol for the predicted global minimum **F0** of the $C_{10}H_8^{+\bullet}(C_6H_6)$ heterodimer and the experimental value of 7.9±1 kcal/mol is excellent.

9

More detailed results on the physical nature of the $C_{10}H_8^{+\bullet}(C_6H_6)$ interaction can be obtained using ALMO-EDA and ALMO-CTA, which partition the interaction energies into four components: a frozen orbital component (FRZ), the polarization (POL), the charge transfer (CT) and the geometric distortion (GEOM). In **Figure 4** we report the fractional contribution of each of these components for the lowest energy member of each class of isomers, as compared to the face-to-face structures of the benzene dimer cation, $(C_6H_6)_2^{+\bullet}$, and the benzene cyclohexane dimer cation, $(C_6H_{12})(C_6H_6)^{+\bullet}$ (optimized and calculated at the same level of theory). The numerical values of each contribution are given in **Table 1**, along with calculated values for the number of electrons transferred. Note that because the ALMO-EDA approach is known to yield lower bounds for the magnitude of charge transfer, conclusions regarding its importance should be robust.[43]
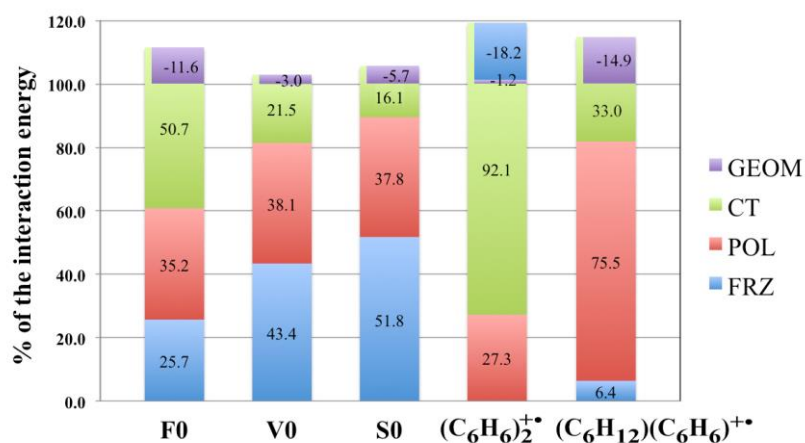

Figure 4. Decomposition of the interaction energies according to ALMO-EDA and ALMO-CTA analyses for the lowest energy isomer of each of the 3 classes identified for $C_{10}H_8^{+\bullet}(C_6H_6)$, as well as results for the benzene dimer cation, and the benzene-cyclohexane cation. Frozen orbital (FRZ), polarization (POL), charge transfer (CT) and geometric distortion (GEOM) components are reported as a percentage of the total interaction energy. A negative percentage thus indicates a repulsive interaction.

Table 1. ALMO-EDA and ALMO-CTA results (M11/cc-pVTZ, in kcal/mol for interaction energy contributions, ΔE, and in m$\bar{e}$ for charge transferred, ΔQ(CT)) for the minimum energy structure within each class for benzene naphthalene dimer cation, compared to the face-to-face structures of the benzene dimer cation, and the benzene cyclohexane dimer cation. The sign convention for ΔE is that positive values are binding.

	F0	V0	S0	$(C_6H_6)_2^{+\bullet}$	$(C_6H_{12})(C_6H_6)^{+\bullet}$
ΔE(FRZ)	2.3	3.8	4.1	-3.0	0.6
ΔE(POL)	3.2	3.3	2.9	4.5	7.1
ΔE(CT)	4.6	1.8	1.3	15.2	3.1
ΔE(GEOM)	-1.0	-0.3	-0.4	-0.2	-1.4
ΔE(**TOT**)	**9.0**	**8.7**	**7.8**	**16.5**	**9.4**
ΔQ(CT)	**63**	**10**	**3**	**420**	**24**

The trends in EDA contributions between isomers can be understood as follows. The frozen orbital term (encompassing dispersion, permanent electrostatics and exchange repulsion) is largest for the face-to-side isomer because of the charge-quadrupole interaction, and smallest for face-to-face. The polarization component, reflecting electron reorganization on the fragments, is quite similar for each class, because of the similar intermolecular spacings. The face-to-face isomers have a very large charge-transfer component that contributes around 50% of the interaction energy, due to the more favorable $\pi_{HOMO}(C_6H_6)$-$\pi_{SOMO}(C_{10}H_8^{+\bullet})$ overlap. Its value is about twice as big as for the V-shaped isomer and over three times larger than for the face-to-side isomer. However, the less favorable frozen interaction means that the overall energy ordering is very close, as discussed already.

In absolute terms, the charge-transfer component is 4.6 kcal/mol for the isomer **F0**, while it is only 1.8 kcal/mol for **V0** and 1.1 kcal/mol for **S0** (**Table 1**). To put the quite large CT contribution of 4.6 kcal/mol for the predicted global minimum **F0** in perspective, it is useful to compare to other related systems (**Table 1**). As a first comparison, the CT contribution to $(C_6H_6)_2^{+\bullet}$ was calculated as 15 kcal/mol for the face-to-face geometry (notice that the frozen orbital term for this system is repulsive). This much larger value reflects the far greater role of CT in a system with zero IP difference between the two components. As a second point of comparison, consider the $(C_6H_{12})(C_6H_6)^{+\bullet}$ dimer, whose interaction energy was characterized experimentally as ΔH^{o}_D = -9.9 kcal/mol.[44] The CT contribution to this interaction energy was calculated as 3.1 kcal/mol, which is noticeably smaller than for $C_{10}H_8^{+\bullet}(C_6H_6)$, as a result of a greater IP difference, and poorer HOMO-SOMO overlap. Nonetheless, the contribution of CT

to $(C_6H_{12})(C_6H_6)^{+\bullet}$ is larger than for the V0 and S0 isomers of $C_{10}H_8^{+\bullet}(C_6H_6)$, where the HOMO-SOMO overlap is even poorer.

The charge transferred between the neutral and the cation is also reported in **Table 1**, using the ALMO-CTA, which is performed in direct analogy to the ALMO-EDA, rather than being a conventional population analysis. The complementary occupied-virtual orbital pair (COVP) that is responsible for the majority of the CT from the neutral fragment (C_6H_6) to the cation fragment ($C_{10}H_8$) in the minimum energy structure for **F0** is also reported in **Figure 5**, and shows the favorable overlap which is responsible for the relatively large charge transfer contribution. The donor occupied level is one of the two $\pi_{HOMO}(C_6H_6)$ levels whilst the acceptor virtual level (related to $\pi_{SOMO}(C_{10}H_8^{+\bullet})$) has adapted to achieve significant overlap. The nature of these orbitals dictates the slipped nature of the **F0** structure, as is clear in Figure 5.
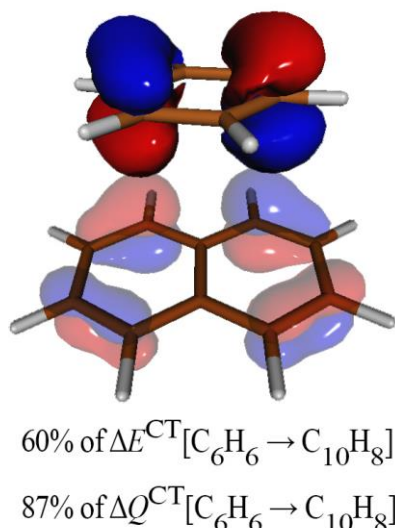

$$60\% \text{ of } \Delta E^{CT}[C_6H_6 \rightarrow C_{10}H_8]$$
$$87\% \text{ of } \Delta Q^{CT}[C_6H_6 \rightarrow C_{10}H_8]$$

Figure 5. The most significant complementary occupied-virtual pair (COVP) in **F0** (isovalue surface of 0.1 a.u.). The donor occupied orbital of the neutral benzene fragment is represented with saturated colors, while the complementary virtual acceptor orbital of the cation fragment is represented in faint colors.

The calculations of the local minima of the $C_{10}H_8^{+\bullet}(C_6H_6)_2$ heterotrimer (the coordinates for the minima are reported in the Supporting Information) show that the global minimum corresponds to the structure where the naphthalene cation is sandwiched between two benzene molecules as shown in **Figure 6**(a). The planes of the molecules are at a slight angle to each other (the angle of intersection between the planes of the benzene molecules and the central naphthalene cation are 8° and 6° respectively), but the structure is essentially

12

analogous to the face-to-face isomer of the $C_{10}H_8^{+\bullet}(C_6H_6)$ heterodimer, with the second benzene stacked on the naphthalene side, slightly displaced from the naphthalene cation. Two higher energy structures of the naphthalene$^{+\bullet}$(benzene)$_2$ trimer were also identified as shown in **Figures 6 (b) and 6(c)**. In structure (b), about 3.5 kcal/mol higher energy than (a), the second benzene molecule attaches to the side of the face-to-face naphthalene$^{+\bullet}$(benzene) dimer forming a slanted U-shaped structure. In structure (c), 4.7 kcal/mol higher energy than (a), the second benzene molecule is attached to the benzene side of the naphthalene$^{+\bullet}$(benzene) dimer forming a parallel benzene dimer stacked to the naphthalene cation. There are undoubtedly numerous other minima, however our unbiased optimization strategy and the experimental findings both suggest that the sandwich structure is likely the global minimum.
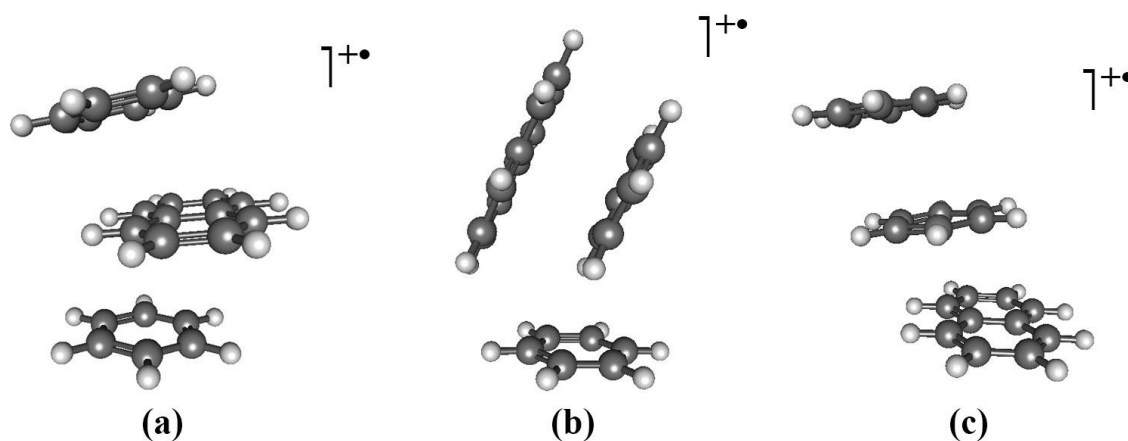
Figure 6. Three isomers of the naphthalene$^{+\bullet}$(benzene)$_2$ heterotrimer: (a) sandwich, (b) slanted U-shaped and (c) parallel stack.

At the most stable geometry, the calculated binding energy of the second benzene molecule to the naphthalene$^{+\bullet}$(benzene) dimer is 9.6 kcal/mol (at 0 K). After thermochemical correction the formation energy is calculated at 9.0 kcal/mol, a value that is 0.6 kcal/mol higher than the calculated binding energy for the first benzene molecule, and is in very good agreement with the 8.4 kcal/mol experimental value obtained from the measured ΔG^o of the association reaction (2). The difference between the binding energies of the first and second benzene molecules is within both experimental and computational uncertainties, but the fact that they are essentially similar is surprising and relatively unusual. One can see this by comparing the formation of $(Bz)_3^{+\bullet}$ from $(Bz)_2^{+\bullet}$ and Bz, where the binding energy of the third

13

benzene molecule in the homotrimer is only 6 kcal/mol vs 17 kcal/mol for the binding energy in the homodimer (M11/cc-pVTZ calculations).

What is the origin of the qualitative difference in the binding of the benzene molecule to $(Bz)_2^{+\bullet}$ in the $(Bz)_3^{+\bullet}$ homotrimer versus the binding to $Naph^{+\bullet}(Bz)$ in the $Naph^{+\bullet}(Bz)_2$ heterotrimer? ALMO-EDA and ALMO-CTA calculations for the two trimer cations (**Table 2**), based on adding the last benzene molecule reveal the origin of the difference. In the $Naph^{+\bullet}(Bz)_2$, heterotrimer, CT is the largest contribution to the interaction energy, and the CTA shows a nearly symmetric transfer of charge to each Bz molecule, leaving 87% of the partial charge on the central $Naph^{+\bullet}$ which is significantly reduced as compared to 97.5% in the dimer. The higher CT from $Naph^{+\bullet}$ to the two benzene molecules in the heterotrimer indicates a strong cooperative effect. By contrast, the ALMO-CTA on the $(Bz)_3^{+\bullet}$ homotrimer reveals that the charge delocalization in this system is much less symmetric. There is a strong CT-dominated interaction between the first two benzenes, and a much weaker interaction with the third benzene molecule, which is polarization-dominated. The polarization effect causes the charge on the central benzene in the $(Bz)_3^{+\bullet}$ homotrimer to *increase* relative to the dimer, the opposite of the case for the $Naph^{+\bullet}(Bz)_2$, heterotrimer.

We calculated the energy for the formation of $(Bz)_3^{+\bullet}$ by the exchange reaction (3) as -18.5 kcal/mol. Of course this route most likely involves an activation barrier, since the neutral benzene has to attack the heterotrimer from the equatorial position to replace the naphthalene moiety sandwiched between the two benzene molecules. Alternatively, the benzene trimer cation $(Bz)_3^{+\bullet}$ could be formed by an exchange reaction involving a higher energy $Naph^{+\bullet}(Bz)_2$ heterotrimer such as **6(c)** where two benzene molecules are stacked above the naphthalene cation. A more detailed analysis of the $Naph^{+\bullet}(Bz)_2$ heterotrimers as compared to the benzene homotrimer cations $(Bz)_3^{+\bullet}$ and their possible formation routes are very interesting problems for potential future investigation.

14

Table 2. ALMO-EDA and ALMO-CTA results (M11/cc-pVTZ, ΔE in kcal/mol, no ZPE corrections, and Q in $\bar{e}$) for the addition of the last benzene molecule to the dimer, to form the benzene naphthalene heterotrimer cation **6(a)**, and the benzene trimer cation $(C_6H_6)_3^{+\bullet}$.

	$C_{10}H_8^{+\bullet}(C_6H_6)_2$	$(C_6H_6)_3^{+\bullet}$
ΔE(FRZ)	2.7	1.0
ΔE(POL)	3.1	3.6
ΔE(CT)	4.1	1.1
ΔE(GEOM)	-0.4	-0.6
Q on the central fragment	0.87	0.71
Q on the left fragment	0.07	0.24
Q on the right fragment	0.06	0.05

In conclusion, the binding energy of the naphthalene$^{+\bullet}$(benzene) heterodimer cation has been determined as 7.9±1 kcal/mol for $C_{10}H_8^{+\bullet}(C_6H_6)$ and 8.1±1 kcal/mol for $C_{10}H_8^{+\bullet}(C_6D_6)$ by equilibrium thermochemical measurements using the mass-selected drift cell technique. Using modern wave function and density functional theory calculations we were able to identify the structures of the minima in the interaction between naphthalene and benzene in the cationic state, and to classify them into three classes: the face-to-face, the V-shaped and the face-to-side isomers. The best method (M11/cc-pVTZ) predicts the lowest energy isomer to have a parallel, face-to-face structure with formation energy of 8.4 kcal/mol in excellent agreement with the experimental results of 7.9-8.1 ±1 kcal/mol. We performed a detailed energetic analysis to understand the nature of the interactions, and to compare the results to the experiment. The stacked face-to-face class of isomers is calculated to have a substantial charge-transfer stabilization (4.6 kcal/mol, about 45% of the total interaction energy) that allows these isomers to have binding energies that are similar, and in many cases higher, than the V-shaped isomers, which have more favorable frozen orbital interaction energies. This unexpectedly high charge-transfer stabilization activates the stacked naphthalene$^{+\bullet}$(benzene)$_2$ heterotrimer to undergo an exchange reaction with a benzene molecule at 219 K to generate the more stable stacked benzene$^{+\bullet}$(benzene)$_2$ homotrimer and a neutral naphthalene molecule.

ASSOCIATED CONTENT

Supporting Information

The experimental setup of the MSIM system (Figure S1), mass spectra for the $C_{10}H_8^{+\bullet}/C_6H_6$ association experiments (Figure S2), interaction energies of the 34 identified isomers of the naphthalene$^{+\bullet}$(benzene) heterodimer cation calculated using the M11/cc-pVTZ method (Table S1), interaction energies of the 15 identified isomers of the

15

naphthalene$^{+\bullet}$(benzene) heterodimer cation calculated at the M06-2X, M11, ωB97X-V, MP2, SCS-MP2 and O2 levels of theory using the cc-pVTZ basis set and at the M11 and ωB97X-V levels using the aug-cc-pVTZ basis set (Table S2), and coordinates for each of the 15 isomers of the naphthalene$^{+\bullet}$(benzene) heterodimer cation, and for the three minima of the naphthalene$^{+\bullet}$(benzene)$_2$ heterotrimer, calculated using the M11/cc-pVTZ method. This material is available free of charge via the Internet at http://pubs.acs.org.

AUTHOR INFORMATION

Corresponding Authors
M. Samy El Shall (mselshal@vcu.edu) and Martin Head-Gordon (mhg@cchem.berkeley.edu)

Notes
The authors declare no competing financial interests.

ACKNOWLEDGEMENT

REFERENCES

1. Badger, B.; Brocklehurst, B. Formation of Dimer Cations of Aromatic Hydrocarbons, *Nature* 1968, 219, 263-263.

2. Enkelmann, V. In *Polynuclear Aromatic Compounds*; *Advances in Chemistry Series*; Ebert, L.B., Ed.; American Chemical Society: Washington, D.C., **1987**; Vol. 217, p 177 and references therein.

3. Hubler, P.; Heinze, J. Kinetic Studies on Reversible Dimerization of Thianthrene and 2,3,7,8-Tetramtoxythianthrene Radical Cations, *Ber. Bunsen. Phys. Chem. Chem. Phys*. **1988**, 102, 1506-1509.

4. Williams, J. M.; Ferraro, J. R.; Thorn, R. J.; Carlson, K. D.; Geiser, U.; Wang, H. H.; Kini, A. M.; Whangbo, M. H. *Organic Superconductors. Synthesis, Structure, Properties and Theory*; Grimes,R. N., Ed.; Prentice Hall: Englewood Cliffs, NJ, **1992**.

5. Kobayashi, H.; Tomita, H.; Naito, T.; Kobayashi, A.; Sakai, F.; Watanabe, T.; Cassoux, P. New BETS Conductors with Magnetic Anions (BETS = nbis(ethylenedithio) tetraselenafulvalene), *J. Am. Chem. Soc.* **1996**, 118, 368-377.

6. Jay K. Kochi, Rajendra Rathore, and Pierre Le Mague`res, Stable Dimeric Aromatic Cation-Radicals. Structural and Spectral Characterization of Through-Space Charge Delocalization, *J. Org. Chem.* **2000**, 65, 6826-6836.

7. Rebek, J., Jr. Assembly and Encapsulation with Self-Complementary Molecules, *Chem. Soc. Rev.* **1996**, 25, 255-264.

8. Fyfe, M. C. T.; Stoddart, J. F. Synthetic Supramolecular Chemistry**,** *Acc. Chem. Res*. **1997**, 30, 339-401.

16

9. Grimme, S. Do Special Non-covalent π-π Stacking Interactions Really Exist?, *Angewandte Chemie Inter. Ed.* **2008**, 47, 3430-3434.

10. Headen, T. F.; Howard, C. A.; Skipper, N. T.; Wilkinson, M. A.; Bowron, D. T.; Soper, A. K. Structure of π-π Interactions in Aromatic Liquids, *J. Am. Chem. Soc.* **2010**, 132, 5735-5742.

11. Rhee, Y. M.; Lee, T. J.; Gudipati, M. S.; Allamandola, L. J. and Head-Gordon, M. "Charged Polycyclic Aromatic Hydrocarbon Clusters and the Galactic Extended Red Emission", *Proceedings of the National Academy of Sciences USA* **2007**, 104, 5274-5278.

12. Iglesias-Groth, S.; Manchado, A.; Garcia-Hernandez, D. A.; Hernandez, J. I. G.; Lambert, D. L. "Evidence for the naphthalene cation in a region of the interstellar medium with anomalous microwave emission", *Astrophys. J. Lett.* **2008**, 685, L55 – L58.

13. Searles, J. M.; Destree, J. D.; Snow, T. P.; Salama, F.; York, D. G.; Dahlstrom, J. "Searching for the Naphthalene Cation Absorption in the Interstellar Medium", *Astrophys. J.* **2011**, 732.

14. Small, D.; Zaitsev, V.; Jung, Y.; Rosokha, S.V.; Head-Gordon, M.; Kochi, J. K. Intermolecular π-to-π Bindings between Stacked Aromatic Dyads. Experimental and Theoretical Binding Energies and NIR Optical Transitions for Phenalenyl Radical/Radical versus Radical/Cation Dimerization. *J. Am. Chem. Soc.* **2004**, 126, 13850-13858.

15. Rusyniak, M.; Ibrahim, Y.; Alsharaeh, E.; Meot-Ner (Mautner), M.; El-Shall, M. S. Mass-selected Ion Mobility Studies of Isomerization of the Benzene Radical Cation and Binding Energy of the Benzene Dimer Cation. Separation of Isomeric Ions by Dimer Formation, *J. Phys. Chem. A.* **2003**, 107, 7656.

16. Meot-Ner (Mautner), M. Dimer Cations of Polycyclic Aromatics. Experimental Bonding Energies and Resonance Stabilization, *J. Phys. Chem.* **1980**, 84, 2724-2728.

17. Meot-Ner (Mautner), M.; El-Shall, M. S. Ionic Charge Transfer Complexes. 1. Cationic Complexes with Delocalized and Partially Localized π Systems, *J. Am. Chem. Soc.* **1986**, 108, 4386-4390.

18. El-Shall, M. S.; Meot-Ner (Mautner), M. Ionic Charge Transfer Complexes. 3. Delocalized π-Systems as Electron Acceptors and Donors. Dimer Cations of Naphthalene Derivatives, *J. Phys. Chem.* **1987**, 91, 1088-1095.

19. Masaki Matsumoto, Yoshiya Inokuchi, Kazuhiko Ohashi, and Nobuyuki Nishi, Charge Delocalization in Benzene−Naphthalene Hetero-Dimer Cation, *J. Phys. Chem. A*, **1997**, *101*, 4574–4578

20. Rusyniak, M.; Ibrahim, Y.; Wright, D.; Khanna, S. and El-Shall, M. S. Gas Phase Ion Mobilities and Structures of Benzene Cluster Cations $(C_6H_6)_n^+$, n = 2-6, *J. Am. Chem. Soc.* **2003**, 125, 12001-12013.

21. Soliman, A. R.; Hamid, A. M.; Abrash, S. A.; El-Shall, M. S. Unconventional Ionic Hydrogen Bonds: $CH^+...\pi$ (C≡C) Binding Energies and Structures of $Benzene^+(Acetylene)_{1-4}$ Clusters, *Chem. Phys. Lett.* **2012**, 523, 25-33.

17

22. Hamid, A. M.; Soliman, A. R.; El-Shall, M. S. Stepwise Association of Hydrogen Cyanide and Acetonitrile with the Benzene Radical Cation: Structures and Binding Energies of $(C_6H_6^{\bullet+})(HCN)_n$, n = 1–6, and $(C_6H_6^{\bullet+})(CH_3CN)_n$, n = 1–4, Clusters, *J. Phys. Chem. A* **2013**, *117*, 1069-1078.

23. Linstrom, P. J.; Mallard, W. G. Eds., NIST Chemistry WebBook, NIST Standard Reference Database Number 69, National Institute of Standards and Technology, Gaithersburg MD, 20899, http://webbook.nist.gov

24. Ohashi, K.; Nishi, N. Photodissociation Spectroscopy of Benzene Cluster Ions $(C_6H_6)_2^+$ and $(C_6H_6)_3^+$, *J. Chem. Phys*. **1991**, 95, 4002-4009.

25. Bornsen, K. O.; Selzle, H. L.; Schlag, E. W. Energy Randomization in the Benzene Dimer Ion, *Chem. Phys. Lett*. **1992**, 190, 497-502.

26. Inokuchi, Y.; Nishi, N. Photodissociation Spectroscopy of Benzene Cluster Ions in Ultraviolet and Infrared Regions: Static and Dynamic Behavior of Positive Charge in Cluster Ions, *J. Chem. Phys*. **2001**, 114, 7059-7065.

27. Ibrahim, Y. M.; Meot-Ner (Mautner), M. and El-Shall, M. S. Associative Charge Transfer Reactions. Temperature Effects and Mechanism of the Gas Phase Polymerization of Propene Initiated by Benzene Radical Cation, *J. Phys. Chem. A*. **2006**, 110, 8585-8592.

28. Momoh, P. O.; Soliman, A. R.; Meot-Ner (Mautner), M.; Rica, A.; El-Shall, M. S. Formation of Complex Organics from Acetylene Catalyzed by Ionized Benzene, *J. Am. Chem. Soc.* **2008**, 130, 12848-12849.

29. Hiraoka, K.; Fujimaki, S.; Aruga, K.; Yamabe, S., Stability and Structure of Benzene Dimer Cation $(C_6H_6)_2^+$, *J. Chem. Phys*.**1991**, 95, 8413.

30. Inokuchi, Y.; Ohashi, K.; Nishi, N. Infrared Photodissociation Spectroscopy of Benzene Trimer Ions. Switching of the Dimer Ion Core in Vibrationally Excited States, *Chem. Phys. Lett*. **1997**, 279, 73-78.

31. Ohashi, K.; Nishi, N. Photodissociation Dynamics of $(C_6H_6)_3^+$: Role of the Extra Benzene Molecule Weakly Bound to the Dimer Core. *J. Chem. Phys*. **1998**, 109, 3971.

32. Iimori, T.; Aoki, Y.; Ohshima, Y. S_1-S_0 Vibronic Spectra of Benzene Clusters Revisited. II. The Trimer, *J. Chem. Phys*. **2002**, 117, 3675-3686.

33. Zhao, Y.; Truhlar, D. G. The M06 Suite of Density Functionals for Main Group Thermochemistry, Thermochemical Kinetics, Noncovalent Interactions, Excited States, and Transition Elements: Two New Functionals and Systematic Testing of Four M06-Class Functionals and 12 Other Functionals. *Theor. Chem. Acc.* **2008**, *120*, 215–241.

34. Peverati, R.; Truhlar, D. G. Improving the Accuracy of Hybrid Meta-GGA Density Functionals by Range Separation. *J. Phys. Chem. Lett.* **2011**, *2*, 2810–2817.

35. Mardirossian, N.; Head-Gordon, M. ωB97X-V: A 10-parameter, Range-separated Hybrid, Generalized Gradient Approximation Density Functional with Nonlocal Correlation, Designed by a Survival-of-the-Fittest Strategy. *Phys. Chem. Chem. Phys.* **2014**, *16*, 9904-9924.

36. Møller, C.; Plesset, M. Note on an Approximation Treatment for Many-Electron Systems. *Phys. Rev.* **1933**, *46*, 0618–0622.

37. Grimme, S. Improved Second-Order Møller–Plesset Perturbation Theory by Separate Scaling of Parallel- and Antiparallel-Spin Pair Correlation Energies. *J. Chem. Phys.* **2003**, *118*, 9095.

38. Lochan, R. C.; Head-Gordon, M. Orbital-Optimized Opposite-Spin Scaled Second-Order Correlation: An Economical Method to Improve the Description of Open-Shell Molecules. *J. Chem. Phys.* **2007**, *126*, 164101.

39. Khaliullin, R. Z.; Cobar, E. A.; Lochan, R. C.; Bell, A. T.; Head-Gordon, M. Unravelling the Origin of Intermolecular Interactions Using Absolutely Localized Molecular Orbitals. *J. Phys. Chem. A* **2007**, *111*, 8753–8765.

40. Horn, P.R.; Sundstrom, E.J.; Baker, T.; Head-Gordon, M. Unrestricted Absolutely Localized Molecular Orbitals for Energy Decomposition Analysis: Theory and Applications to Intermolecular Interactions Involving Radicals. *J. Chem. Phys.* **2013,** 138, 134119.

41. Khaliullin, R. Z.; Bell, A. T.; Head-Gordon, M. Analysis of Charge Transfer Effects in Molecular Complexes Based on Absolutely Localized Molecular Orbitals. *J. Chem. Phys.* **2008**, *128*, 184112.

42. Shao, Y.; Gan, Z.; Epifanovsky, E.; Gilbert, A. T. B.; Wormit, M.; Kussmann, J.; Lange, A. W.; Behn, A.; Deng, J.; Feng, X.; et al. Advances in Molecular Quantum Chemistry Contained in the Q-Chem 4 Program Package. *Mol. Phys.* **2014**, DOI:10.1080/00268976.2014.952696.

43. Azar, R.J.; Horn, P.R.; Sundstrom, E.J.; Head-Gordon, M. Useful Lower Limits to Polarization Contributions to Intermolecular Interactions using a Minimal Basis of Localized Orthogonal Orbitals: Theory and Analysis of the Water Dimer. *J. Chem. Phys.* **2013,** 138, 084102

44. Meot-Ner (Mautner), M.; Hamlet, P.; Hunter, E. P.; Field, F. H. Bonding Energies in Association Ions of Aromatic Compounds. Correlations with Ionization Energies, *J. Am. Chem. Soc.* **1978**, 100, 5466-5471.

19